HHS Public Access

Author manuscript

*Nat Med*. Author manuscript; available in PMC 2016 May 01.

Published in final edited form as:

*Nat Med*. 2015 November ; 21(11): 1337–1343. doi:10.1038/nm.3957.

# Selective inhibition of the p38 alternative activation pathway in infiltrating T cells inhibits pancreatic cancer progression

**Muhammad S. Alam**[1,7], **Matthias M. Gaida**[1,2,7], **Frank Bergmann**[2], **Felix Lasitschka**[2], **Thomas Giese**[3], **Nathalia A. Giese**[4], **Thilo Hackert**[4], **Ulf Hinz**[4], **S. Perwez Hussain**[5], **Serguei V. Kozlov**[6], and **Jonathan D. Ashwell**[1,*]

[1]Laboratory of Immune Cell Biology, Center for Cancer Research, National Cancer Institute, National Institutes of Health

[2]Institute of Pathology, University Hospital Heidelberg, Germany

[3]Institute of Immunology, University of Heidelberg, Germany

[4]Department of Surgery, University Hospital Heidelberg, Germany

[5]Pancreatic Cancer Unit, Laboratory of Human Carcinogenesis, Center for Cancer Research, National Cancer Institute, National Institutes of Health

[6]Cancer and Developmental Biology Laboratory, National Cancer Institute at Frederick, National Institutes of Health

## Abstract

Pancreatic ductal adenocarcinoma (PDAC) is a highly aggressive neoplasm characterized by a marked fibro-inflammatory microenvironment[1], the presence of which can promote both cancer induction and growth[2–4]. Therefore, selective manipulation of local cytokines is an attractive if unrealized therapeutic approach. T cells possess a unique mechanism of activation of p38 MAPK downstream of T cell receptor (TCR) engagement by phosphorylation of Tyr-323 (pY323). This alternative p38 activation pathway is required for pro-inflammatory cytokine production[5,6]. Here we show in human PDAC that a high percentage of infiltrating $pY323^+$ T cells was associated with large numbers of TNFα and IL-17-producing $CD4^+$ tumor-infiltrating lymphocytes (TIL) and aggressive disease. The growth of murine pancreatic tumors was inhibited by genetic ablation of the alternative p38 pathway, and transfer of wild type $CD4^+$ T cells but not those lacking the



*Correspondence should be addressed to J.D.A. (jda@pop.nci.nih.gov).

[7]These authors contributed equally to this work and are listed in alphabetical order.

**AUTHOR CONTRIBUTIONS**

M.S.A. and M.M.G. contributed equally to this manuscript and are listed in alphabetical order. M.S.A., M.M.G., and J.D.A. designed the experiments, analyzed the data, and wrote the manuscript. M.S.A. and M.M.G. performed all mouse and in vitro experiments. M.M.G. did the tissue evaluation and the computer-based tissue analysis. F.B. provided human paraffin tissues, created the human tissue microarray, performed the corresponding immunohistochemistry, and evaluated tissue samples together with M.M.G. F.L. performed and analyzed multicolor-immunofluorescence staining of human tissues, and T.G., N.A.G., and T.H. collected fresh frozen tissues, performed qPCR, and provided the patient clinical data. S.P.H. and S.V.K. screened and provided KPC mice. S.V.K. and U.H. performed biostatistics and mulitvariate analysis of human data.

**COMPETING FINANCIAL INTERESTS**

The authors declare no competing financial interests.

alternative pathway enhanced tumor growth in T cell-deficient mice. Strikingly, a plasma membrane-permeable peptide derived from Gadd45α, the naturally-occurring inhibitor of p38 pY323$^+$ (ref. 7), reduced CD4$^+$ TIL production of TNFα, IL-17A, IL-10, and secondary cytokines, halted growth of implanted tumors, and inhibited progression of spontaneous K-ras-driven adenocarcinoma in mice. Thus, TCR-mediated activation of CD4$^+$ TIL results in alternative p38 activation and production of pro-tumorigenic factors, and can be targeted for therapeutic benefit.

A hallmark of PDAC is a fibro-inflammatory microenvironment that is a major source of tumor-promoting cytokines and chemokines, causing angiogenesis, metastasis, resistance to chemotherapeutic agents, and escape from host defenses[8–10]. Consistent with this, anti-inflammatory treatment of in mice with PDAC has been shown to reduce the development of precancerous lesions, tumor vascularization, and cancer growth[11,12]. Infiltrating T cells are a prominent feature of the inflammatory microenvironment and can be a source of tumor-promoting cytokines[2–4]. Given that the p38 alternative activation pathway is upstream of many such T-cell cytokines[6,13], its involvement in human PDAC was evaluated. Pancreatic tissues were collected from 192 histologically-classified primary PDAC patients that had not had neoadjuvant therapy at the time of surgery and were analyzed for infiltrating p38 pY323$^+$ T cells. In all samples there was infiltration of T cells that stained with antibodies to pY323 p38. Histological examination of sequential serial sections revealed the presence of CD3$^+$ T cells expressing both p38 pY323 and TNF-α (Supplementary Fig. 1a). Triple-immunofluorescence staining revealed the presence of p38 pY323$^+$ cells expressing both TNF-α and IL-17A (Fig. 1a). Enumeration of the percentage of pY323$^+$ TIL allowed us to segregate patients into two groups based on receiver operating characteristic (ROC) analysis: those with less than 10% (mean: 4.3%) CD3$^+$pY323$^+$ tumor-infiltrating T cells (n=153, ~80%) and those with ≥ 10% (n=39, mean: 15.5%) (Fig. 1b). Of note, although there was no difference in the degree of CD3$^+$ T cell infiltration between the two groups (Fig. 1b), the percentage of TNF-α-, IL-17A-, and IL-21-producing CD4$^+$ T cells was much higher in the subset of patients with ≥ 10% pY323$^+$ p38 T cells (Fig. 1c and Supplementary Fig. 1b). The expression of the Th17 transcription factor *Rorc* and the proangiogenic factor *Vegf* (a factor downstream of TNF-α and IL-17A) (Fig. 1d) and correspondingly the density of CD31-positive tumor vessels, which is associated with poor prognosis[14] (Fig. 1e), was increased in the high pY323$^+$ p38 group. However, expression of the T helper and regulatory cell transcription factors *Gata3*, *Tbet*, and *Foxp3* was similar between the two groups (Supplementary Fig. 1c). Recent studies have shown that PDAC can be subclassified based upon tumor plasticity, in which an epithelial phenotype changes towards a mesenchymal phenotype, epithelial-mesenchymal transition (EMT). These cells lose epithelial markers (cytokeratin 19) and acquire mesenchymal markers (α-smooth muscle actin, vimentin, desmin) and EMT promoters (sonic hedgehog, snail, CCL20, leptin)[15,16]. We found no differences in EMT markers between the two groups (Supplementary Fig. 1d). Importantly, patients having infiltrates with ≥ 10% pY323$^+$ p38 T cells had a statistically-significantly poorer prognosis (median survival 9.8 months; 5.3% 5-year survival) compared to patients with <10% pY323$^+$ p38 cells (median survival 20.3 months; 16.1% 5-year survival) (Fig. 1f). No correlations with other clinical or pathological findings (age, gender, tumor size, TNM classification stage, histological grading, status of resection margin, or number of tumor positive lymph nodes) were found (Supplementary

Table 1). Multivariate Cox-regression analysis confirmed that the prevalence of p38 pY323$^+$ TIL is an independent prognostic marker for PDAC (Supplementary Table 2). When patients with incurable disease at the time of surgery (e.g. liver metastases or residual macroscopic cancer) were excluded, CD4$^+$ T cell p38 pY323 status remained an independent prognostic factor (Supplementary Table 3).

The finding that p38 pY323$^+$ CD4$^+$ TIL are a feature of aggressive human PDAC prompted us to investigate how the T cell p38 alternative pathway affects tumor progression in two different murine models of pancreatic cancer. We injected Panc02 pancreatic tumor cells subcutaneously into the flank of WT mice or animals in which Tyr-323 in p38α and β is replaced with Phe (double knock-in, or DKI mice). The latter have intact stress- but not TCR-induced p38 activity, and have diminished TCR-induced production of pro-inflammatory cytokines *in vitro* and *in vivo* [13]. Notably, Panc02 tumors in DKI mice had reduced volume and weight compared to WT animals (Fig. 2a). This was not due to decreased T cell infiltration (Supplementary Fig. 2a) or CD4$^+$ T cell activation as assessed by cell surface CD44 and CD69 expression (Supplementary Fig. 2b). However, many more WT than DKI CD4$^+$ TIL produced TNFα (Fig. 2b). In addition, the number of CD4$^+$ TIL producing IL-10, another tumor-promoting cytokine[17], was lower in DKI mice (Fig. 2b). WT and DKI mice had small and similar numbers of T cells producing INFγ at low levels, and IL-17 was found at very low levels in CD4$^+$ TIL from both genotypes. TNFα is downstream of the transcription factor IRF4[18], which itself is downstream of alternative p38 activation[6], and there was a corresponding reduction in IRF4 expression in DKI CD4$^+$ TIL (Supplementary Fig. 2c). The percentage of TNF-α-producing CD8$^+$ TIL from WT mice was low compared to CD4$^+$ TIL, and was modestly reduced further in DKI mice (Supplementary Fig. 2d). Notably, TNFα production by tumor-infiltrating macrophages, B cells, granulocytes, and myeloid-derived suppressor cells was similar between WT and DKI mice (Supplementary Fig. 2e). DKI CD4$^+$ TIL stimulated via the TCR produced less TNF-α than WT TIL, whereas the response of both to PMA and ionomycin was similar (Supplementary Fig. 2f). To determine whether T-cell mediated enhancement of tumor growth was in fact due to CD4$^+$ T cell-derived TNFα, we adoptively transferred transferred CD4$^+$ T cells from WT or *Tnf*-deficient mice to *Tcra*$^{-/-}$ mice, and 10 days later we injected Panc02 cells subcutaneously. Despite equivalent T cell engraftment (Supplementary Fig. 3a), tumors grew more rapidly in recipients of WT T cells (Fig. 2c). Adoptive transfer of CD4$^+$, but not CD8$^+$, WT, or DKI T cells into *Tcra*$^{-/-}$ hosts followed by tumor cell inoculation showed that the differences in tumor growth were CD4$^+$ T-cell-intrinsic (Fig. 2d and Supplementary Fig. 3b). In addition to its direct effects on tumor cell growth and viability, TNF-α induces the expression of cytokines and chemokines with protumorigenic activity from tumor cells[19]. Consistent with a decrease in TNFα production by CD4$^+$ TIL, tumor cells from DKI mice had markedly reduced expression of *Ccl2*, which induces tumor cell migration and neoangiogenesis, and the proangiogenic factor *Vegf*, whereas *Ccl5* and *Tgfβ* were unaffected (Fig. 2e). Correspondingly, although T cell infiltration was similar, the density of tumor microvessel formation as indicated by CD31 staining was reduced in DKI tumors (Fig. 2f). Panc02 cells express TNFR1 and TNFR2 (data not shown), and given that TNF-α directly induced *Ccl2* and *Vegf* in Panc02 cells in vitro (Fig. 2g) and that TNF-α

production was only elevated in infiltrating T cells (Fig. 2b and Supplementary Fig. 2e), we propose that expression of *Vegf* and *Ccl2 in vivo* was in response to T cell-derived TNFα.

We examined a second tumor model using KPC mice that express mutated K-ras in pancreatic epithelium, and when heterozygous for p53 develop spontaneous tumors starting at approximately 8–10 weeks of age that closely mimic the human disease, including pancreatic intraepithelial neoplasia precursor lesions (PanIN) and progression to fully-developed carcinoma[20]. In regions rich in infiltrating T cells we easily detected $CD3^+$ mononuclear cells that stained for both pY323 p38 and TNF-α, which were absent in T cell-poor regions (Fig. 2h and Supplementary Fig. 3c; isotype control in Supplementary Fig. 3d). To ask if alternative p38 activation was involved in oncogene-driven tumorigenesis, 6-week old KPC mice were lethally irradiated and reconstituted with WT or DKI bone marrow. The former developed invasive cancer and had a median survival of 28 days (mean survival of 37±9 days), whereas mice that received DKI bone marrow survived much longer (median survival 84 days, mean survival 80±16 days) (Fig. 2i). Therefore, the p38 alternative pathway promotes tumor progression in orthotopic and genetic models of murine pancreatic cancer, in agreement with the finding that large numbers of p38 $pY323^+$ TIL in human cancer are associated with aggressive disease.

Given the genetic evidence that ablating the T-cell restricted p38 alternative pathway impairs tumor-promoting cytokine production, we developed a selective inhibitor of this pathway. Gadd45α binds p38 and inhibits the activity of pY323 (alternatively activated) but not pT180/pY182 (classically activated) p38 (ref. 7). To determine the minimum p38-interacting fragment, Gadd45α residues 71–96, which bind p38 (ref. 21), and overlapping subregions were fused with GST and used to pull down recombinant p38. GST-71–96 pulled down p38 as did GST-71–85, whereas 81–96 could not (Fig. 3a). In agreement, Gaddd45α in which amino acids 71–80 were deleted (Gadd45αΔ10) bound p38 poorly (Fig. 3b). GST-Gadd45α and GST-71–85 completely blocked phosphorylation of ATF2 by Zap70 (alternatively)-activated p38, whereas Gadd45αΔ10 had no effect (Fig. 3c). Importantly, neither Gadd45α nor its fragments affected phosphorylation of ATF2 by MKK6 (classically)-activated p38. Thus, the highly conserved Gadd45α residues 71–85 specifically inhibit the activity of pY323 p38.

The addition of multiple arginine residues can promote cellular uptake of proteins as large as ~50 kDa[22,23]. We created a recombinant molecule containing 11 N-terminal arginines followed by Gadd45α fragment 71–85 ((11R) 71–85), which was still able to inhibit Zap70-activated p38 (Fig. 3d). The uptake and longevity of FITC-labeled (11R) 71–85 was measured by flow cytometry (Fig. 3e). After a 2 hr incubation all cells were FITC-bright, with the signal decaying over the next 24–48 hr. The ability of (11R) 71–85 to inhibit p38 activation in T cells was determined by the phosphorylation of ATF2, a substrate common to both the alternative and classical pathway. (11R) 71–85 inhibited the phosphorylation of p38 in anti-CD3/CD28-stimulated but not PMA/ionomycin-stimulated T cells (Fig. 3f). (11R) 71–85 inhibited anti-CD3/CD28-induced T cell proliferation in a dose-dependent manner but had no effect on B cells (Fig. 3g), which lack the alternative pathway[5]. (11R) 71–85 inhibited anti-CD3/CD28- but not PMA/ionomycin-induced T cell proliferation over a range of stimulatory concentrations (Fig. 3h) without affecting cell viability (Supplementary Fig.

4). (11R) 71–85-treated $CD4^+$ T cells produced much less TNF-α than controls in response to anti-CD3/CD28, the inhibition being similar to that caused by the p38 catalytic inhibitor SB203580 (Fig. 3i). In contrast, whereas SB203580 inhibited TNFα induced by PMA/ionomycin, (11R) 71–85 had no effect. Thus, (11R) 71–85 targets alternatively- but not classically-activated p38. Notably, (11R) 71–85 had no effect on Th1 or cytotoxic T cell (CTL) effector function, as measured by IFNγ production by Th1-skewed $CD4^+$ T cells and $CD8^+$ CTL degranulation and production of IFNγ, respectively (Supplementary Fig. 5a and b).

To test the therapeutic potential of (11R) 71–85, WT mice were inoculated with Panc02 s.c. and tumors were allowed to grow for 14 days. The tumors were injected with (11R) Scr, (11R) 71–85, or water 3 times a week. Whereas tumor growth progressed in mice treated with controls, it was inhibited by (11R) 71–85 (Fig. 4a). The specificity of (11R) 71–85 was confirmed by the finding that it had no effect on tumor growth in DKI mice (Supplementary Fig. 6a). Histopathological analysis showed less vascularization (CD31 staining) in (11R) 71–85-treated tumors (Fig. 4b). In agreement with the findings in DKI mice, $CD4^+$ TIL from (11R) 71–85-treated tumors produced less TNF-α than those from control-treated animals, whereas the amount of IFNγ was relatively unaffected (Supplementary Fig. 6b). (11R) 71–85 itself had no effect on Panc02 growth and viability in vitro (Supplementary Fig. 6c), and histological examination of tumors showed no elevation of tumor cell apoptosis or necrosis (Supplementary Fig. 6d,e). Consistent with a cytostatic effect, tumors in (11R) 71–85-treated mice resumed growth when administration of the peptide ceased (Fig. 4a, **left panel**). Importantly, there was no toxicity associated with (11R) 71–85, as judged by the condition and weight of the mice, and normal serum levels of alanine aminotransferase, aspartate aminotransferase, alkaline phosphatase, amylase, and lactate dehydrogenase, intracellular enzymes that are released by tissue damage (Supplementary Fig. 6f).

We next treated KPC mice with (11R) 71–85 or (11R) Scr starting at 9 weeks of age and evaluated the pancreas 3.5 weeks later. The area of intrapancreatic fibro-inflammatory reaction was reduced in (11R) 71–85-treated compared to (11R) Scr-treated mice (Fig. 4c), and the area of normal pancreas was higher in the former (Fig. 4d). Correspondingly, (11R) 71–85 slowed progression to late PanIN (PanIN3, carcinoma *in situ*) and adenocarcinoma but not initiation (early PanIN), and was associated with reduced acinar-to-ductal metaplasia (ADM) that did not, however, reach statistical significance (Fig. 4d). Eight of 16 mice treated with (11R) Scr developed PDAC, 5 of which died during the course of treatment due to progressive cancer (31.2%) (Table 1). In contrast, only 14.2% (2 of 14) of mice treated with (11R) 71–85 developed PDAC, one of which died (7.1%). Pancreata from KPC mice treated with (11R) 71–85 had statistically significant reductions in the numbers of $CD4^+$ T cells expressing TNF-α, the Th17 transcription factor RORγt, IL-17A, and IL-10 compared to controls, with the number of cells expressing IFNγ being only slightly reduced (Fig. 4e, the gating strategy is shown in Supplementary Fig. 6g). In line with reduced TNF-α, (11R) 71–85 decreased *Irf4* and *Rorc* mRNA expression in $CD4^+$ TIL (Supplementary Fig. 6h). To investigate the particular effector T helper cell types secreting TNF-α and affected by (11R) 71–85, we stained TIL from KPC mice for TNF-α and the Th type-specific transcription factors Gata3 and RORγt. Although a small percentage of TNF-α-producing Th2 and Th17

cells were observed, neither were major producers (Supplementary Fig. 6i). (11R) 71–85 also inhibited factors downstream of TNF-α such as *Ccl2*, *Ccl5*, *Vegf*, and *Tgfβ* in pancreatic cells (Fig. 4f). Treatment of KPC mice was begun at 9 weeks of age, when the pancreas was expected to be largely normal. To ask if (11R) 71–85 could affect pre-existing tumors, a survival study was done using mice with verified pancreatic tumors. KPC mice in which tumors were confirmed by ultrasound (volumes 100–150 $mm^3$) were randomized into two groups, one receiving (11R) 71–85 and the other (11R) Scr intravenously three times a week. There was a clear and statistically significant difference in survival between these groups, with the control mice living a median of 10 days (mean survival 12 ± 3 days) and the treated mice a median of 20 days (mean survival 22 ± 4 days) ($P < 0.05$) (Fig. 4g). The effect of (11R) 71–85 on production of pro-inflammatory factors in established tumors was determined after 3 injections. As with the prevention model, there was a reduction in the percent of $CD4^+$ TIL producing TNF-α, RORγt, and IL-17A, and IFNγ was decreased in both $CD4^+$ and $CD8^+$ TIL (Supplementary Fig. 7a and b). Interestingly, treatment with (11R) 71–85 increased the ratio of $CD8^+$ to $CD4^+$ T cells in the tumor, which has been associated with decreased disease (Supplementary Fig. 7c)[24,25]. These results support the possibility that inhibition of the alternative p38 pathway could be useful both as a neoadjuvant (preoperative) and adjuvant therapy.

Nearly all solid tumors have infiltrating immune cells that are unable to eliminate the tumor and in many cases paradoxically promote tumor progression by creating a microenvironment with features of chronic inflammation[2–4,10,26–28]. One tumor-promoting cytokine in the micromilieu is TNF-α, and anti-TNF-α therapies have been beneficial in treating cancer [29,30]. In addition, it was recently shown that Th17 cells enhanced the progression of PanIN[31], supporting the notion that T cells are promising targets in inflammatory cancers. Given its central role in cytokine production, one might expect that inhibiting p38 would be beneficial in inflammatory diseases or cancers[32]. However, to date all selective p38 catalytic inhibitors have failed due to side effects such as liver toxicity, presumably because of off-target activities or global p38 inhibition[33]. The latter might be avoided if one could specifically target T cell p38. In this report, inhibition of T cell-derived inflammatory cytokines with a cell membrane-permeable Gadd45α-derived peptide inhibited neoangiogenesis, PanIN, and PDAC progression. Many of the pro-tumorigenic factors in the neoplastic milieu (e.g. CCL2, CCL5, VEGF, and TGFβ) are not T cell-derived[2,4,19,34], and it is therefore notable that specific inhibition of T cell p38 resulted in their decline. This indicates that infiltrating T cells orchestrate the production of tumor-promoting factors from non-T cells, even tumor cells themselves.

Therapeutic strategies are moving toward “personalized oncology”, the targeting of often complex differences in the molecular bases for tumor initiation and progression between individuals. In this regard, we found that the presence of a high percentage of p38 $pY323^+$ TIL is a very strong negative prognostic factor in human PDAC, and that interference with this pathway in murine PDAC was beneficial in both preventive and treatment models. Therefore, interference with the p38 alternative pathway with selective compounds such as (11R) 71–85 may be of particular benefit to patients with high levels of p38 $pY323^+$ TIL. A potential advantage of targeting the T cell p38 alternative pathway in the tumor

microenvironment, rather than a single cytokine or factor, is that it interferes with multiple downstream pro-inflammatory events involved in tumor progression.

## ONLINE METHODS

### Mice

Wild type (WT) C57BL/6 (B6) mice were obtained from Frederick Cancer Research Facility (Frederick, MD). Mice expressing p38αβ$^{Y323F}$, in which endogenous p38α and p38β contain a Tyr -> Phe substitution at residue 323 (double knockin, or DKI mice)[13], were crossed onto the B6 background for at least 12 generations. TCRα$^{-/-}$ mice were obtained from Jackson Laboratories. Healthy eight to twelve week old age and sex matched mice were used for experiments. To obtain KPC mice, conditional *LSL-Trp53$^{R172H/+}$ LSL-Kras$^{G12D/+}$* were interbred with *Pdx-1-Cre* mice to yield *LSL-Kras$^{G12D/+}$;LSL-Trp53$^{R172H/+}$;Pdx-1-Cre* triple mutant animals. Mice were maintained in the National Cancer Institute pathogen-free facility. All animal experiments were performed under animal study protocols approved by the National Cancer Institute Animal Care and Use Committee.

### 11R-fused peptides

The amino acid sequences of the murine Gadd45α-derived peptide ((11R) 71–85) and the scrambled control ((11R) Scr) were RRRRRRRRRRRLQIHFTLIRAFCCEN and RRRRRRRRRRRRNECICIQLTFHAFL, respectively. The lyophilized peptides were purchased from Peptide 2.0 and reconstituted as recommended by the manufacturer.

### Reagents

The following antibodies were used to detect murine proteins: p38α (5F11; Cell Signaling), FcR (2.4G2; BD Biosciences), TCRβ (H57-597; eBiosciences), CD4 (RM4-5; BD Biosciences), CD8 (53-6.7; BD Biosciences), B220 (RA3-6b; BD), CD11b (M1/70; BD), CD44 (IM7; BD), CD69 (H1.2F3; BD), F4/80 (BM8; eBiosciences), Gr1 (RB6-8C5; eBiosciences), MHC class II (M5 1114.15.2 ; eBiosciences), TNF-α (MP6-XT22; eBiosciences), TNFR1 (AF-425-PB; R&D systems), and IFNγ (XMG1.2; eBiosciences). GST was detected with B-14 (Santa Cruz Biotechnology). Live/dead cell discrimination was performed with Aqua or UV live/death fixable stain (Molecular Probes) and apoptosis detected with Annexin V (51-65875X; BD). Recombinant mouse TNF-α was purchased from Gibco (PMC3014). Anti-CD3 (145-2C11) and anti-CD28 (37.51) were purchased from BD Pharmingen. Phorbol myristate acetate (PMA) and ionomycin were purchased from Sigma-Aldrich. Recombinant active Zap70 protein (Cat#N12-30G) was purchased from R&D Systems. DNAse I was purchased from Sigma and Liberase from Roche. [γ-$^{32}$P]ATP was purchased from Perkin Elmer. For mouse immunohistochemistry, the DakoEnvision kit was used (DAKO) along with the antibodies to CD3 (16669), CD31 (28364), and TNF-α (6671), purchased from abcam. For human immunohistochemistry and immunofluorescence, anti-CD3 (SP7, Labvision; PS1 Santa Cruz), anti-CD4 (polyclonal IgG, abcam), anti-CD31 (JC10A) from Dako, anti-TNFα (2C8, abcam), anti-IL17A (AF-317-NA, R&D Systems), anti-IL-21 (ab53655, abcam) were used. Anti-p38 pY323 (PP3411) was purchased from ECM Biosciences. Isopropyl β-D-thiogalactopyranoside was purchased from Sigma.

Chelating- and Glutathione-Sepharose Fast Flow beads were purchased from Amersham Biosciences.

### Panc02 cells

The mouse pancreatic cancer B6 cell line Panc02 (a gift from Jack Greiner, NCI; mycoplasma-free) was grown in RPMI containing 10% fetal calf serum supplemented with penicillin/streptomycin and L-glutamine (complete medium) at 37°C in 5% $CO_2$.

### T-cell purification

T cells were purified using mouse T cell recovery column kits (Cederlane). For positive selection of $CD4^+$ T cells, mouse $CD4^+$ T cell isolation kit II was used (Myltenyi).

### In vitro T-cell assays

$5 \times 10^4$ purified T cells in 200 μl (proliferation) or $5 \times 10^5$ purified T cells in 2 ml (Western blotting) of complete medium were stimulated with plate-bound anti-CD3 (2 μg/ml) and anti-CD28 (2 μg/ml) or PMA (10 ng/ml) and ionomycin (1 μg/ml) for 48 hr. To measure proliferation, [$^3$H]-thymidine was added and the cells were harvested 16 h later. Cell culture supernatants were collected after 48 h and TNF-α detected by ELISA (Ready-Set-Go kit, eBiosciences).

### Adoptive transfer

For adoptive transfer experiments, $CD4^+$ or $CD8^+$ T cells were isolated from spleens and lymph nodes of WT, DKI, and TNF-$\alpha^{-/-}$ donor mice to more than 90% purity. $2.5 \times 10^6$ cells/300 μl PBS were injected into the tail vein of recipient mice. After ten days, $7.5 \times 10^5$ Panc02 cells were inoculated in the left flank and tumor growth was monitored.

### Protein expression and purification

p38α, MKK6, and Gadd45α proteins were expressed in the bacterial strain BL21(DE3) using the vectors pGEX-4T-1 or pET15b. The 10 amino acid internal deletion mutation of Gadd45α (G45αΔ71–80) was generated by site-directed mutagenesis using the QuikChange kit (Stratagene). For the synthesis of small peptide fragments of Gadd45α, oligonucleotides were synthesized, annealed, and ligated to the pGEX-4T-1 vector. After plasmid transformation, single colonies were grown in culture, and after reaching an $A_{600}$ of 0.5–1.0 protein expression was induced with 0.5 mM isopropyl β-D-thiogalactopyranoside. Cultures were further incubated at 14°C overnight. Cells were resuspended in PBS (including 0.5 M NaCl if His-tagged), 0.1% Triton X-100, and 1 mM phenylmethylsulfonyl fluoride, sonicated, and centrifuged at 20,000 × g at 4°C for 20 min. His-tagged proteins were purified with cobalt-charged chelating-Sepharose Fast Flow beads and eluted with 0.3 M imidazole in PBS with 0.5 M NaCl. GST-tagged proteins were purified with Glutathione-Sepharose Fast Flow beads and eluted with 50 mM Tris, pH 8, containing 20 mM glutathione. Proteins were concentrated and washed into PBS using Microcon YM-30 spin columns (Millipore).

### Protein pull-downs

Recombinant p38 was incubated with GST beads coated with Gaddd45α FL or fragments in PBS at 37°C for 1 hr, at which time beads were washed with PBS and analyzed for p38 and GST levels by Western blot using antibodies against p38 and GST.

### In vitro kinase (IVK) assays

Recombinant p38 was activated with ZAP70 or MKK6 at 30°C for 1 hr or left unactivated in IVK buffer (20 mM Tris, pH 7.5, 10 mM $MgCl_2$, 2 mM dithiothreitol, 5 mM β-glycerophosphate, 5 mM NaF, and 0.2 mM $Na_3VO_4$). After 1 hr, Gadd45α full-length (G45αFL), 71–85 amino acid peptide fragment (G45α (71–85)), the 10 amino acid Gadd45α internal deletion (G45αΔ71–80), or 11R-fused peptides were added at the indicated concentrations and incubated at 30°C for another 20 min. ATF-2 was added for a final 30 min in the presence of 10 μCi [$\gamma$-$^{32}$P] ATP.

### LCMV infection and CTL assay

LCMV Armstrong 53b was grown in baby hamster kidney cells, and viral titers determined[35]. B6 mice were infected i.p. with $2 \times 10^5$ PFU and splenocytes were harvested at day 8. Cells were treated as indictated and stimulated with LCMV gp33 and gp276 for 5 hr in the presence of 1 μM monensin. Cells were stained for CD107a and IFNγ and analyzed by flow cytometry.

### Bone marrow chimeras

Six week old KPC mice were treated with oral antibiotics for one week and then irradiated with 9 Gy. Mice were reconstituted with $10^7$ T cell-depleted (Dynabeads, Invitrogen) bone marrow cells from WT or DKI mice.

### Isolation and stimulation of TIL, tumor cells, pancreas infiltrating T cells, and pancreatic cells

Panc02 tumors or pancreata were explanted and minced into 1–2 mm pieces followed by incubation in HBSS containing DNAse I and Liberase for 30 min, and pressed once through a 70 μm strainer and twice through a 40 μm strainer (BD Falcon) to create single cell suspensions. $10^6$ cells were cultured in monensin alone or together with PMA and ionomycin or with anti-CD3/CD28-coated plates at 37°C for 4 h. Some mice were injected with Brefeldin A (0.25 mg in 0.5 ml of PBS) 6 h before harvesting and intracellular staining for cytokines. $CD4^+$ T cells from single cell suspensions of Panc02 tumors or KPC pancreata were isolated using $CD4^+$ positive selection. In some experiments, Panc02 cells from established tumors or pancreatic cells from KPC mice were isolated pressing through a 70 μm strainer followed by Lympholyte M gradient centrifugation.

### Flow cytometry

One million cells were incubated with anti-FcR and cell surface staining performed with the indicated antibodies for 30 min on ice. For intracellular staining, cells were washed in FACS buffer (1% BSA plus 0.1% sodium azide), fixed, and permeabilized with Cytofix/Cytoperm solution for 25 min on ice followed by washing in Perm/Wash solution (BD Biosciences).

Cells were stained for an additional 30 min at room temperature with the indicated antibodies. All antibodies were used at a dilution of 1:100. Panc02 tumor cells were stained with a goat anti-mouse TNFR1 followed by FITC labeled anti-goat. In all experiments cell survival was determined with Aqua or UV live/death fixable stain. Apoptosis was detected in some experiments by staining with PE-Annexin V. Flow cytometry was performed using an LSRII with FACSDiva software (BD Biosciences), and data were analyzed with FlowJo 9.2 software (TreeStar).

### Real-time PCR

Total RNA was isolated using Qiagen RNeasy Kits and was reverse transcribed using Omniscript RT kit (Qiagen) according the manufacturer's instructions. Power Sybr Green premix (Applied Biosystems) was used for quantitative PCR. All data were normalized to HPRT (hypoxanthine-guanine phosphoribosyl transferase) RNA and are presented as expression relative to this control. The primers were: CCL2-Fwd: CCCAATGAGTAGGCTGGAGA, CCL2-Rev: TCTGGACCCATTCCTTCTTG; CCL5-Fwd: ATATGGCTCGGACACCACTC, CCL5- Rev: TCCTTCGAGTGACAAACACG; VEGFa-Fwd: GTGAGGTTTGATCCGCATGAT, VEGFa-Rev: GACCCTGGCTTTACTGCTGTA; TGFβ-Fwd: TTGCTTCAGCTCCACAGAGA, TGFβ-Rev: TGGTTGTAGAGGGCAAGGAC; IRF4-Fwd: GCAGCTCACTTTGGATGACA, IRF4-Rev: CCAAACGTCACAGGACATTG; Hprt-Fwd: AGCCTAAGATGAGCGCAAGT, Hprt-Rev: TTACTAGGCAGATGGCCACA.

### Gene expression analysis in human tumor tissue

Tissue samples were collected and stored in RNAlater (Ambion). Tissues were disrupted with the RiboLyser device (ThermoHYBAID, Heidelberg) in 400 µl lysis buffer from the MagnaPure mRNA Isolation Kit I containing 1% DTT (v/w) (ROCHE Diagnostics). Three hundred µl of the lysate were collected and mixed with 120 µl lysis buffer containing DTT. After centrifugation at 13000 rpm for 5 min, the mix was transferred into a MagnaPure sample cartridge and mRNA was isolated with the MagnaPure-LC device using the their protocol for cells. An aliquot of 8.2 µl mRNA was reversely transcribed using AMV-RT and oligo- (dT) as primer (First Strand cDNA synthesis kit, Roche) in a thermocycler. After termination of the cDNA synthesis, the reaction mix was diluted to a final volume of 500 µl. Primer sets optimized for the LightCycler® (RAS) were developed and purchased from SEARCH-LC GmbH (www.Search-LC.com). PCR was performed with the LightCycler® FastStart DNA Sybr GreenI kit (RAS) according to the protocols provided in the parameter-specific kits. To control for specificity of the amplification products, a melting curve analysis was performed. The copy number was calculated from a standard curve, obtained by plotting known input concentrations of four different plasmids at log dilutions to the PCR-cycle number (CP) at which the detected fluorescence intensity reached a fixed value. The calculated transcript numbers were normalized to the expression of the housekeeping gene peptidylprolyl isomerase B (PPIB).

### MTT (3-(4,5-dimethylthiazol-2-yl)-2,5-diphenyltetrazolium bromide) assay

$10^4$ Panc02 cells were seeded overnight and incubated with different concentrations of recombinant mouse TNF-α, (11R) 71–85, or (11R) Scr with appropriate vehicle controls. The MTT assay was performed according to the manufacturer's instructions (Cayman).

### Histology and immunohistochemistry

Mouse tumors or pancreata were explanted, fixed in formalin, embedded in paraffin, and 4 μm consecutive tissue sections made. Prior to antibody incubation, heat pre-treatment using citrate buffer (pH 6.1) was performed. CD3 T cells were counted in 5 representative 400x high power fields, CD31-positive vessels were counted at 200x. Quantification of PanIN was made by microscopic analysis of 80 representative pancreatic ducts in H&E stained sections. The scoring of murine PanIN was performed as described[36]. In addition, software-based imaging was performed and the histological features (normal pancreas, fibroinflammatory infiltrate, acinar-ductal-metaplasia (ADM), early PanIN, and late PanIN) were quantitated. Slides were scanned at 400x using an Aperio CS scanner and stored in the Aperio svs file format, using JPEG and JPEG2000 compression in eSlide Manager (Aperio), and evaluated using ImageScope Software (Aperio). Apoptosis were detected with the ApopTag Peroxidase In Situ Apoptosis Detection Kit (Millipore). The groups were coded and all histological scoring was performed by two double-blinded experienced observers. Photos were made using an AxioVison (Zeiss). A tissue microarray containing 193 samples of pancreatic tissue from patients diagnosed with PDAC was made in the clinical routine diagnostic at the University Hospital of Heidelberg. The study was approved by the local ethics committee of the University of Heidelberg and a written informed consent of each patient was taken. The diagnosis of PDAC and the tumor stage were established according to the criteria recommended by the World Health Organization[37] and the UICC[38]. Primary pancreatic cancer tissues were used from patients who underwent surgical resection without any neoadjuvant therapy. The tissue was stained with an automated immunostaining system (Ventana). All infiltrated CD3-positive T cells (including tertiary lymphoid structures) were counted in 5 representative HPF, and the percentage of pY323-positive cells among CD3 positive cells was counted in direct serial sections of the array spots. The cutoff of 10% for the pY323 high and low group was empirically determined according to the mean values of the amount of p38 pY323-positive T cells (mean: 0–10% $CD3^+$ $pY323^+$: 4.3%; mean: ≥ 10% $CD3^+$ $pY323^+$: 15.5%). For vascular density, 10 samples of the p38 pY323 low (0–10%) and high (≥ 10%) groups were randomly selected and stained with anti CD31, and the number of $CD31^+$ vessels was counted in 5 representative HPF from each sample. Software-based quantitate was performed as above. The study was approved by the Ethics Committee of the University of Heidelberg and a written informed consent was obtained from all the patients.

### Immunofluorescence staining

Immunofluorescence staining was performed on 2 μm paraffin sections of formalin-fixed tissues. Antigen retrieval was achieved by steam cooking the slides in 1 mM EDTA (pH 8, Dako) for 30 min. 10% Earle's balanced salt solution supplemented with 1% HEPES and 0.1% saponin at pH 7.4 was used as washing buffer. Antibodies against TNF-α (1:50), p38

pY323 (1:50), CD3 (1:50), CD4 (1:50) were used with isotype-matched controls as well as normal rabbit Ig (Dako, Dianova, R&D) and incubated at room temperature for 1 hr. Biotinylated donkey anti-rabbit IgG Ab (1:200, Jackson Immunolaboratories), goat anti-mouse IgG1 Ab (1:100, Jackson Immunolaboratories), and sheep anti-mouse IgG Ab, (Binding Site, 1:250) were used as secondary antibodies at room temperature for 30 min, followed by Cy-3-conjugated streptavidin (1:1000, red fluorescence, Jackson Immunolaboratories), Cy5-conjugated donkey anti-rabbit Ab, (1:200, cyan fluorescence, Jackson Immunolaboratories), or DyLight488-conjugated donkey anti-sheep antibody (1:200, green fluorescence; Jackson Immunolaboratories) for 30 min. Slides were mounted with a 4′,6-diamidino-2-phenylindole (DAPI)-containing mounting medium (Roti-Mount FluorCare DAPI; Roth). Slides were viewed in 400x magnification with a Laserscan microscope using suitable filter combinations provided by the manufacturer (Leica Microsystems). 250 tumor-infiltrating $CD3^+$ and $CD4^+$ lymphocytes were counted in different areas of each tumor and the percentage of TNF-$\alpha^+$ cells was calculated.

## KPC mouse enrollment for treatment, monitoring, and endpoints

For the prevention experiments, apparently healthy 9 week old KPC of either sex were randomized into the treatment ((11R) 71–85; 11 male, 3 female) or control ((11R) Scr; 12 male, 4 female) group. For the treatment studies, male KPC animals were monitored by weekly palpation for the presence of abdominal masses. Mice with suspected pancreatic lesions were further evaluated by ultrasound imaging to confirm tumor presence, linear dimensions, and anatomic location within the pancreas. Based on the imaging data, 3D volumes were computed for each tumor, and lesions were qualified as residing in the head of pancreas (HOP), body of pancreas (BOP) or tail of pancreas (TOP). Only tumors consistent with PDAC appearance, lacking cystic or significant inflammatory components, and measuring less than 150 $mm^3$ in volume were considered enrollable and assigned by a stratified randomization algorithm to one of two study arms using a rolling enrollment approach, based on tumor baseline volume, individual animal weight and age at enrollment. Mice with two or more distinct tumors detected in pancreas, tumor masses detected in other sites/organs, as well as animals displaying signs of biliary occlusion (as e.g. evidenced by an enlarged gall bladder), or overall poor health were excluded from further consideration. Mice were treated with 80 μg/200 μl of either (11R) 71–85 or (11R) Scr in PBS/3% acetonitrile three times per week on alternate days for up to 6 weeks. Animals were monitored twice daily, and mice deemed moribund were euthanized and necropsied. The sample sizes were chosen to be sufficient to allow statistical analysis of the outcomes of the experimental *versus* control arms of the studies.

## Ultrasound

Prior to the scan mice were shaved and a depilatory (Surgi-Cream, Surgi-Care) applied to remove fine hair and reduce image artifacts due to air/transducer interface. Prior to imaging, 3 ml of saline were injected i.p. to float the pancreas and improve image contrast with respect to surrounding organs. Warm ultrasound gel was applied to reduce image artifacts at the transducer-skin interface. The acoustic focus was placed at the center of the pancreatic tumor. Images were acquired in 3D using the Vevo2100 ultrasound scanner (VisualSonics, Inc, Toronto, Canada), MS-550S transducer (40 μm axial resolution) at 40 MHz with 0.076

mm step size (image thickness). Tumor volumes were analyzed using the parallel ROI algorithm (Vevo2100 VisualSonics software).

### Treatment plan, monitoring, and study endpoints

Animals were dosed with 80 μg/200 μl of either experimental or control peptide (formulated in PBS/3% acetonitrile) for three days per week on alternate days for up to 6 weeks. Animals were monitored twice daily for signs of deteriorating health as indicated by weight loss, slow movement, hunched posture, and hypothermia. Mice deemed morbid by the above criteria were processed by terminal blood plasma collection, followed by a full necropsy and tissue preservation for histopathologic and biomarker evaluation. Animals were imaged mid-treatment, at day 13, and whenever possible, at day 27. Stat imaging was applied for animals that reached the study endpoint prior to the scheduled imaging date.

### Statistical analyses

Statistics were calculated using Graph.Pad Prism 6.0 software with the appropriate statistical tests: two tailed Student's t-test, one sample t-test (tumor weight, hypothetical value 100), and Wilcoxon-signed Rank (MTT assay, hypothetical value 100). $p<0.05$ (*), $p<0.01$(**), $p<0.001$(***). SAS software (Release 9.4, SAS institute, Cary; NC, USA) was used for survival analyses. The Kaplan-Meier method was performed to estimate survival rates and the log-rank test was used to compare survival curves statistically. For multivariate survival analysis the Cox proportional hazards model was used to compute hazard ratios and its 95% confidence interval. ROC curves were calculated to determine the pY323 cutoff for long-term survival by using logistic regression analysis. Correlations between the two groups (high vs. low pY323) and clinical or pathological findings were analyzed by using the Fisher's exact test and the Mann-Whitney-U test. All tests were used two-sided and a p-value $<0.05$ was considered as statistical significant.

## Supplementary Material

Refer to Web version on PubMed Central for supplementary material.

## Acknowledgments

The authors thank Jutta Scheuerer, Mona Clauter, Bettina Walter, and Ehydel Castro for expert technical assistance, Jack Greiner for Panc02 cells, the CAPR program at the Frederick National Laboratory for Cancer Research for providing KPC mice for some studies, Thomas Longerich and Bernd Lahrmann for technical advice in computer-based tissue analysis, and Peter Schirmacher for critical review of the manuscript. This work was supported by the Intramural Research Program of the Center for Cancer Research, National Cancer Institute, National Institutes of Health. M.M.G. was supported by a fellowship from the German Research Foundation (DFG) Ga-1818/1-1. The work of F.L. was in part funded by the German Research Foundation, SFB 938/TP Z2.

## References

1. Neesse A, et al. Stromal biology and therapy in pancreatic cancer. Gut. 2011; 60:861–868. [PubMed: 20966025]
2. Coussens LM, Zitvogel L, Palucka AK. Neutralizing tumor-promoting chronic inflammation: a magic bullet? Science. 2013; 339:286–291. [PubMed: 23329041]
3. Mantovani A, Allavena P, Sica A, Balkwill F. Cancer-related inflammation. Nature. 2008; 454:436–444. [PubMed: 18650914]

4. Grivennikov SI, Greten FR, Karin M. Immunity, inflammation, and cancer. Cell. 2010; 140:883–899. [PubMed: 20303878]
5. Salvador JM, et al. Alternative p38 activation pathway mediated by T cell receptor-proximal tyrosine kinases. Nat Immunol. 2005; 6:390–395. [PubMed: 15735648]
6. Alam MS, et al. Counter-regulation of T cell effector function by differentially activated p38. J Exp Med. 2014; 211:1257–1270. [PubMed: 24863062]
7. Salvador JM, Mittelstadt PR, Belova GI, Fornace AJJ, Ashwell JD. The autoimmune suppressor Gadd45alpha inhibits the T cell alternative p38 activation pathway. Nat Immunol. 2005; 6:396–402. [PubMed: 15735649]
8. Steele CW, et al. Exploiting inflammation for therapeutic gain in pancreatic cancer. Br J Cancer. 2013; 108:997–1003. [PubMed: 23385734]
9. Kleeff J, et al. Pancreatic cancer microenvironment. Int J Cancer. 2007; 121:699–705. [PubMed: 17534898]
10. Ozdemir BC, et al. Depletion of carcinoma-associated fibroblasts and fibrosis induces immunosuppression and accelerates pancreas cancer with reduced survival. Cancer Cell. 2014; 25:719–734. [PubMed: 24856586]
11. Rao CV, et al. Inhibition of pancreatic intraepithelial neoplasia progression to carcinoma by nitric oxide-releasing aspirin in p48(Cre/+)-LSL-Kras(G12D/+) mice. Neoplasia. 2012; 14:778–787. [PubMed: 23019409]
12. Mayorek N, Naftali-Shani N, Grunewald M. Diclofenac inhibits tumor growth in a murine model of pancreatic cancer by modulation of VEGF levels and arginase activity. PLoS One. 2010; 5:e12715. [PubMed: 20856806]
13. Jirmanova L, Giardino Torchia ML, Sarma ND, Mittelstadt PR, Ashwell JD. Lack of the T cell-specific alternative p38 activation pathway reduces autoimmunity and inflammation. Blood. 2011; 118:3280–3289. [PubMed: 21715315]
14. Takagi K, Takada T, Amano H. A high peripheral microvessel density count correlates with a poor prognosis in pancreatic cancer. J Gastroenterol. 2005; 40:402–408. [PubMed: 15870976]
15. Collisson EA, et al. Subtypes of pancreatic ductal adenocarcinoma and their differing responses to therapy. Nat Med. 2011; 17:500–503. [PubMed: 21460848]
16. Mathew E, et al. Dosage-dependent regulation of pancreatic cancer growth and angiogenesis by hedgehog signaling. Cell Rep. 2014; 9:484–494. [PubMed: 25310976]
17. Liu CY, et al. M2-polarized tumor-associated macrophages promoted epithelial-mesenchymal transition in pancreatic cancer cells, partially through TLR4/IL-10 signaling pathway. Lab Invest. 2013; 93:844–854. [PubMed: 23752129]
18. Raczkowski F, et al. The transcription factor Interferon Regulatory Factor 4 is required for the generation of protective effector CD8+ T cells. Proc Natl Acad Sci U S A. 2013; 110:15019–15024. [PubMed: 23980171]
19. Ben-Baruch A. The Tumor-Promoting Flow of Cells Into, Within and Out of the Tumor Site: Regulation by the Inflammatory Axis of TNFalpha and Chemokines. Cancer Microenviron. 2012; 5:151–164. [PubMed: 22190050]
20. Hingorani SR, et al. Trp53R172H and KrasG12D cooperate to promote chromosomal instability and widely metastatic pancreatic ductal adenocarcinoma in mice. Cancer Cell. 2005; 7:469–483. [PubMed: 15894267]
21. Bulavin DV, Kovalsky O, Hollander MC, Fornace AJJ. Loss of oncogenic H-ras-induced cell cycle arrest and p38 mitogen-activated protein kinase activation by disruption of Gadd45a. Mol Cell Biol. 2003; 23:3859–3871. [PubMed: 12748288]
22. Noguchi H, et al. A new cell-permeable peptide allows successful allogeneic islet transplantation in mice. Nat Med. 2004; 10:305–309. [PubMed: 14770176]
23. Matsushita M, et al. A high-efficiency protein transduction system demonstrating the role of PKA in long-lasting long-term potentiation. J Neurosci. 2001; 21:6000–6007. [PubMed: 11487623]
24. Zhang Y, et al. CD4+ T lymphocyte ablation prevents pancreatic carcinogenesis in mice. Cancer Immunol Res. 2014; 2:423–435. [PubMed: 24795355]

25. Sato E, et al. Intraepithelial CD8+ tumor-infiltrating lymphocytes and a high CD8+/regulatory T cell ratio are associated with favorable prognosis in ovarian cancer. Proc Natl Acad Sci U S A. 2005; 102:18538–18543. [PubMed: 16344461]
26. Lin WW, Karin M. A cytokine-mediated link between innate immunity, inflammation, and cancer. J Clin Invest. 2007; 117:1175–1183. [PubMed: 17476347]
27. Park EJ, et al. Dietary and genetic obesity promote liver inflammation and tumorigenesis by enhancing IL-6 and TNF expression. Cell. 2010; 140:197–208. [PubMed: 20141834]
28. Grivennikov SI, et al. Adenoma-linked barrier defects and microbial products drive IL-23/IL-17-mediated tumour growth. Nature. 2012; 491:254–258. [PubMed: 23034650]
29. Egberts JH, et al. Anti-tumor necrosis factor therapy inhibits pancreatic tumor growth and metastasis. Cancer Res. 2008; 68:1443–1450. [PubMed: 18316608]
30. Waterston AM, et al. TNF autovaccination induces self anti-TNF antibodies and inhibits metastasis in a murine melanoma model. Br J Cancer. 2004; 90:1279–1284. [PubMed: 15026813]
31. McAllister F, et al. Oncogenic Kras activates a hematopoietic-to-epithelial IL-17 signaling axis in preinvasive pancreatic neoplasia. Cancer Cell. 2014; 25:621–637. [PubMed: 24823639]
32. Waetzig GH, Seegert D, Rosenstiel P, Nikolaus S, Schreiber S. p38 mitogen-activated protein kinase is activated and linked to TNF-alpha signaling in inflammatory bowel disease. J Immunol. 2002; 168:5342–5351. [PubMed: 11994493]
33. Wagner EF, Nebreda AR. Signal integration by JNK and p38 MAPK pathways in cancer development. Nat Rev Cancer. 2009; 9:537–549. [PubMed: 19629069]
34. Germano G, et al. Role of macrophage targeting in the antitumor activity of trabectedin. Cancer Cell. 2013; 23:249–262. [PubMed: 23410977]
35. Dutko FJ, Oldstone MB. Genomic and biological variation among commonly used lymphocytic choriomeningitis virus strains. J Gen Virol. 1983; 64:1689–1698. [PubMed: 6875516]
36. Hingorani SR, et al. Preinvasive and invasive ductal pancreatic cancer and its early detection in the mouse. Cancer Cell. 2003; 4:437–450. [PubMed: 14706336]
37. Bosman, FT.; Carneiro, F.; Hruban, RH.; Theise, ND. World Health Organisation classification of tumours. Pathology and genetics of tumours of the digestive system. IARC Press; Lyon: 2010.
38. Sobin, LH.; Gospodarowicz, MG.; Wittekind, C. TNM classification of malignant tumours. JohnWiley & Sons; Oxford: 2009.

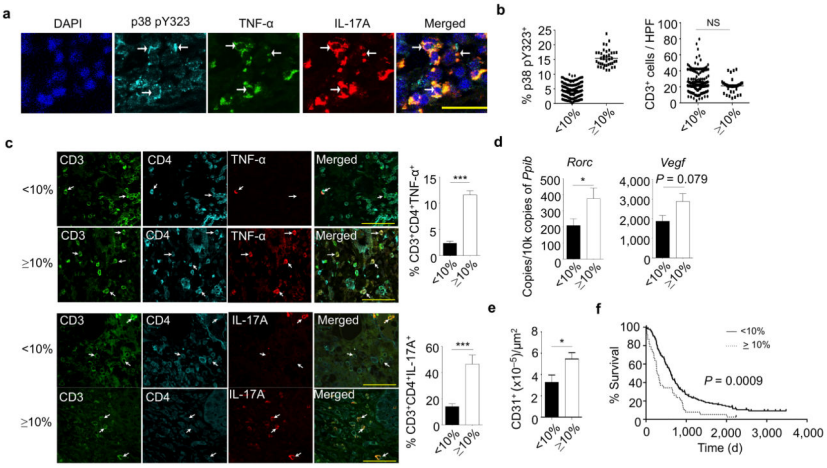


**Figure 1. A high percentage of pY323$^+$ p38 TIL is associated with enhanced pro-inflammatory cytokine production and shorter survival in human PDAC**

(**a**) Triple-immunofluorescence of PDAC tissue was performed for p38 pY323 (cyan), TNF-α (green), and IL-17A (red). DAPI was used to stain the nucleus. Examples of positive cells are denoted with arrows.

(**b**) Human PDAC sections were stained for CD3 and the percentage of p38 pY323$^+$ cells and the absolute number of CD3$^+$ cells was determined in samples from patients with low (<10%, n=153) *versus* high (≥10%, n=39) percentages of p38 pY323$^+$ TIL (NS=not significant, nonparametric Mann-Whitney test).

(**c**) Triple-immunofluorescence of PDAC from patients with <10% *versus* ≥10% pY323$^+$ p38 T cells for CD3 (green), CD4 (cyan), and TNF-α (red) or IL-17A (red) (left panel). Examples of positive cells are denoted with arrows. The percentage of CD3$^+$CD4$^+$ cells expressing TNF-α or IL-17 is shown on the right (n=10 patients per group, *** $P < 0.001$, nonparametric Mann-Whitney test). Histogrames represent means ± SEM.

(**d**) Quantitative RT-PCR of the expression of *Rorc* (n=16 patients per group) and *Vegf* (n=14 patients per group) in PDAC tissue lysates (* $P < 0.05$, nonparametric Mann-Whitney test). Histograms represent means ± SEM.

(**e**) Vascular density (CD31$^+$) of patient samples with <10% (n=10) *versus* ≥10% (n=10) pY323$^+$ p38 T cells (* $P < 0.05$, nonparametric Mann-Whitney test). Histograms represent means ± SEM.

(**f**) Correlation of patient survival with the percentage of pY323$^+$ p38 TIL (<10%, n=153; ≥10%, n=39) ($p$=0.0009, determined by Log-rank test).

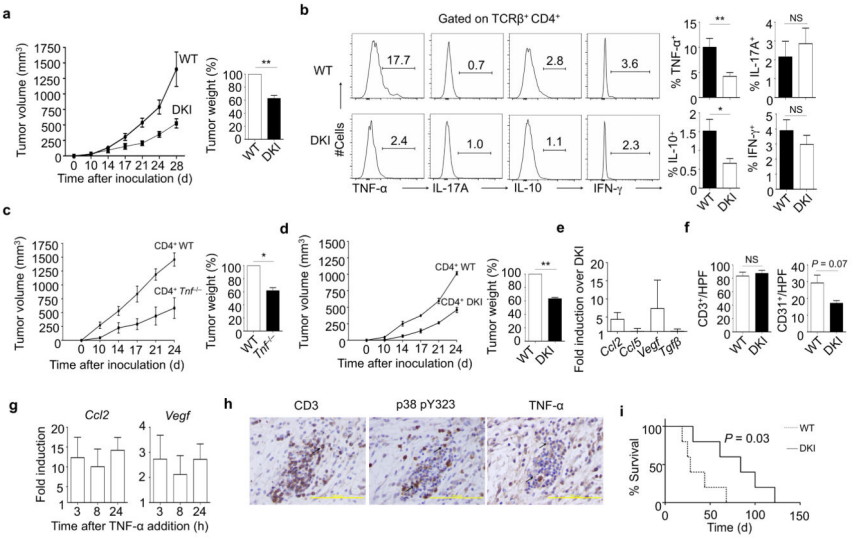

**Figure 2. CD4$^+$ T cell activated by the p38 alternative pathway promotes growth of pancreatic cancer**

(**a**) Panc02 tumor cells were injected in the flank of WT (n=17) or DKI (n=16) mice and tumors monitored over time (left), and tumor weight as a percent of WT was determined at day 28 (right) (** $P < 0.01$, one sample t-test).

(**b**) Tumor-infiltrating TCRβ$^+$CD4$^+$ T cells from WT and DKI mice were analyzed on day 28 for expression of TNF-α (WT, n=14, DKI, n=13), IFNγ (WT, n=15, DKI, n=15), IL-10 (WT, n=15, DKI, n=15), and IL-17A (WT, n=8, DKI, n=9) (left histograms). ** $P < 0.01$, * $P < 0.05$, NS=not significant, nonparametric Mann-Whitney test.

**(c)** Purified CD4$^+$ T cells from WT or *Tnf*$^{-/-}$ mice were adoptively transferred into *Tcra*$^{-/-}$ mice. Ten days later, Panc02 tumor cells were injected in the flank and tumors monitored over time (left) and tumor weight as a percent of WT was determined at day 24 (right) (n=3 per group; * $P < 0.05$, one sample t-test).

(**d**) As in **c**, except CD4$^+$ T cells from DKI mice were used for adoptive transfer (n=3 mice per group; ** $P < 0.01$, one sample t-test).

(**e**) Panc02 cells were isolated from WT or DKI mice (n=4 per group) at day 28 and analyzed for *Ccl2*, *Ccl5*, *Vegf*, and *Tgfβ* by quantitative real-time PCR.

(**f**) Immunohistochemical staining for tumor-infiltrating T cells (CD3) and tumor microvessels (CD31) in WT and DKI mice. The results of multiple experiments were averaged (n=6 mice per group; NS=not significant, nonparametric Mann-Whitney test). Results shown in **Fig. a–f** represent the mean ± SEM.

(**g**) Panc02 cells were cultured for the indicated times with 10 ng/ml mouse recombinant TNF-α and analyzed for *Ccl2* and *Vegf* mRNA expression by quantitative real-time PCR. Results are the mean ± SD of two independent experiments.

**(h)** Immunohistochemical staining of serial sections of a KPC pancreatic tumor. Examples of TIL positive for CD3, p38 pY323, and TNF-α are denoted with arrows. The figures are representative of sections from 8 mice.

(**i**) KPC mice were irradiated with 9 Gy at 6 weeks of age, reconstituted with $10^7$ WT or DKI bone marrow cells, and monitored for survival (n=5 mice per group; * $P < 0.05$, Log-rank test).

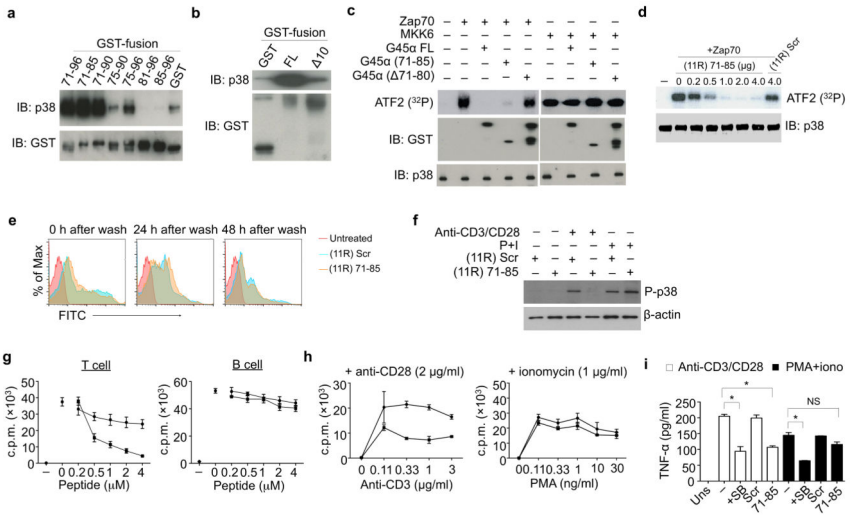


**Figure 3. Gadd45α residues 71–85 bind p38 and inhibits T cell proliferation and effector function**

(**a, b**) Recombinant soluble p38 was incubated with beads coated with full length Gadd45α (G45α FL) and the indicated fragments in PBS at 37°C for 1 hr. Eluates were immunoblotted for p38 and GST. Results are representative of two independent experiments.

(**c**) Recombinant p38 was activated with Zap70, MKK6, or IVK buffer alone at 30°C for 1 hr, then incubated with the indicated GST-Gadd45α fusion proteins at 30°C for 20 min. ATF2 was added with 10 μCi [γ-$^{32}$P] ATP for an additional 30 min. $^{32}$P incorporation was detected by SDS-PAGE and autoradiography. Results are representative of two independent experiments.

(**d**) Recombinant p38 was phosphorylated by Zap70 or IVK buffer alone and then incubated with (11R) 71–85 or (11R) Scr at 30°C for 20 min. ATF2 was added with 10 μCi [γ-$^{32}$P] ATP for an additional 30 min, and $^{32}$P incorporation was assessed. Results are representative of two independent experiments.

(**e**) Purified B6 splenic T cells were incubated or not with FITC-labeled (11R) 71–85 or (11R) Scr for 2 hr. Cells were washed and analyzed at the indicated times for retention of the fluorescently-labeled peptides. Results are representative of two independent experiments.

(**f**) Purified T cells were incubated as in **e**, then stimulated with plate-bound anti-CD3/CD28 or PMA/ionomycin for 1 hr, lysed, and immunoblotted for phospho-p38 (P-p38). Results are representative of three independent experiments.

(**g**) Purified T or B cells were incubated in **e** and stimulated with plate-bound anti-CD3/CD28 (T cells) or anti-IgM-Fab$_2$′ (B cells) for 48 hr. [$^3$H]-thymidine was added 16 hr before cells were harvested. Results are representative of three independent experiments.

(**h**) Freshly purified T cells were incubated as in **e**, then stimulated with the indicated amounts of plate-bound anti-CD3 and a fixed amount of plate-bound anti-CD28 or the indicated concentrations of PMA and a fixed concentration of ionomycin for 48 hr. [$^3$H]-thymidine was added 16 hr before cells were harvested. Results are representative of three independent experiments.

(**i**) Purified T cells were incubated or not with (11R) 71–85 or (11R) Scr as in **e,** then stimulated with anti-CD3/CD28 or PMA and ionomycin for 48 hr before collecting the supernatants and measuring TNF-α by ELISA. Results are representative of three independent experiments.

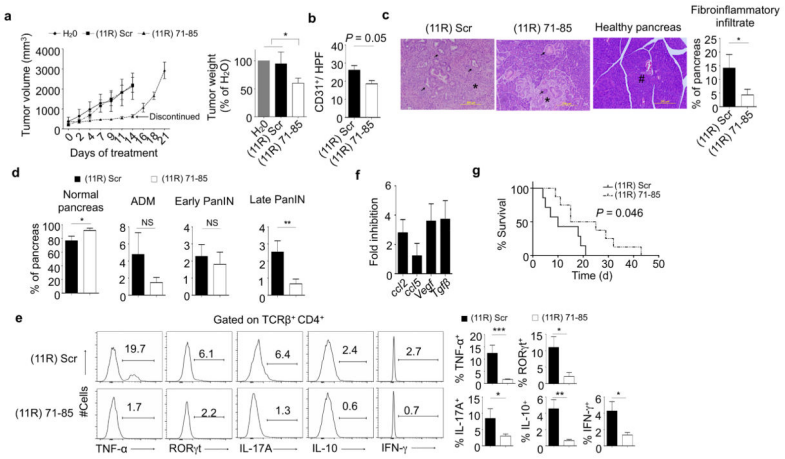


**Figure 4. (11R) 71–85 inhibits tumor growth, angiogenesis, PanIN progression, and invasive cancer in mice**

(**a**) Panc02 cells were injected into B6 mice and allowed to grow to an estimated volume of 300 $mm^3$. Intratumor injections were performed 3 times a week with $H_20$, (11R) Scr, or (11R) 71–85 for 2 weeks and tumors (n=3 $H_20$ and (11R) Scr, n=8 (11R) 71–85). Tumor weight was assessed at day 14. For three (11R) 71–85 injected mice, treatment was stopped after 2 weeks and tumor growth monitored. (* $P < 0.05$, one sample t-test).

(**b**) B6 mice were inoculated with Panc02 cells and treated as in **a**. Immunohistochemical staining for detection of tumor microvessels (CD31) was performed 24 hr after the last injection. The average of (11R) Scr (n=5) and (11R) 71–85 (n=6) is shown ($P = 0.05$, nonparametric Mann-Whitney test).

(**c**) Nine-week old KPC mice were given (11R) 71–85 (n=13) or (11R) Scr (n=11) three times a week for 3.5 weeks, at which time H&E-stained pancreatic sections were analyzed. Arrows indicate PanIN, arrowheads indicate invasive cancer, asterisks indicate fibroinflammatory stroma, and the hash symbol indicates a normal pancreatic duct. The quantification of fibroinflammatory infiltrate is shown on the right (* $P < 0.05$, nonparametric Mann-Whitney test).

(**d**) Quantification of normal ducts, ADM, early PanIN, late PanIN, and PDAC in KPC mice treated as in **c**.

(**e**) Infiltrating $TCR\beta^+CD4^+$ T cells from mice treated as in **c** were analyzed for intracellular TNF-α ((11R) Scr, n=10; (11R) 71–85, n=11), RORγt (n=6 mice per group), IL-17A (n=8 mice per group), IL-10 ((11R) Scr, n=6; (11R) 71–85, n=8, and IFNγ (n=5 mice per group) (histograms). Bar graphs show the mean ± SEM. (*** $P < 0.001$, ** $P < 0.01$, * $P < 0.05$, NS=not significant, nonparametric Mann-Whitney test).

(**f**) KPC mice were treated as in **c** and the expression of the indicated genes was analyzed in isolated pancreatic epithelial cells by quantitative real-time PCR (n=6 mice for (11R) Scr and 3 mice for (11R) 71–85).

(**g**) KPC mice with confirmed pancreatic tumors were treated with either (11R) 71–85 (n=8) or (11R) Scr (n=7) i.v. 3 times per week and their survival followed. The *P* value was determined by the Mantel-Cox method.

## Table 1

PDAC occurrence in KPC mice after (11R) Scr or (11R) 71–85 treatment

| | Treatment | |
|---|---|---|
| | **(11R) Scr** | **(11R) 71–85** |
| PDAC | 8/16 (50%) | 2/14 (14.3%) |
| Macroscopic | 6 | 1 |
| Microscopic | 2 | 1 |

The incidence of PDAC in the KPC mice used in Fig. 4c after 3.5 weeks of treatment.